

## Chapter 4

### Electrical transport properties of metallic glasses

#### 4.1 Introduction

The study of the electrical transport properties of amorphous metallic alloys has unearthed many new phenomena and has necessitated a paradigm shift to explain the contrast between crystalline and amorphous metallic systems.

A detailed review of the study of electrical transport properties of metallic glasses has been given by K.V. Rao [1]. Unlike crystalline metallic systems which generally show a positive temperature coefficient of resistance, amorphous metallic alloys can show either a positive or a negative temperature coefficient of resistance. An empirical correlation between the magnitude of the resistivity and the sign of the temperature coefficient of resistance (TCR) was first noticed by Mooij [2] in 1973. He found that metallic glasses with a resistivity greater than  $150 \mu\text{ohm cm}$  have a negative temperature coefficient, while those with a resistivity below this value show a positive temperature coefficient. A natural explanation of the Mooij correlation can be given on the basis of the modified Ziman's theory [3].

Metallic glasses which are strongly magnetic show both positive and negative temperature coefficients over different temperature ranges. Some of them show a minimum at a temperature slightly below the Curie temperature. These effects might have a magnetic origin and require a treatment different from that of other metallic glasses.

#### 4.2 Ziman's theory of Liquid metals

Since the disorder in a glass maybe comparable to that in a liquid, it was thought that the theory of J.M.Ziman [4], which was used to explain the resistivity of liquid metals could be extended to the case of metallic glasses with certain modifications.

The original Ziman theory deals with the potential scattering of conduction electrons by a disordered set of scattering centers. In simple single element metallic liquids, these scattering centers are represented by pseudopotentials. In the framework of the Ziman approach, the temperature dependence of the resistivity is governed by that of the interference function or the structure factor  $s(k)$ . In such a model, the magnitude as well as the temperature coefficient of the resistivity of an alloy would be determined by the relative position of  $2k_F$ , where  $k_F$  is the fermi-momentum vector, with respect to  $k_p$ , the position of the first peak in the structure factor  $s(k)$ . The dynamic effects appear through the Debye-Waller factor that describes the temperature dependence of  $s(k)$ .

The basic Ziman theory was extended by Evans et al [5] to transition metal liquid alloys by replacing the pseudopotential matrix element with a t-matrix in order to incorporate scattering phase shifts for non-overlapping potentials. The diffraction model expression for the resistivity of a pure liquid metal is

$$\rho = \frac{24\pi^2\Omega_o}{e^2hv_f} \int s(k)|t(k)|^2\left(\frac{k}{k_F}\right)^3d\left(\frac{k}{k_F}\right) \quad (4.1)$$

Where  $k_F$  and  $v_F$  are the wave-vector and velocity of the electrons at the Fermi surface.  $t(k)$  is the scattering matrix and  $\Omega_o$  is the atomic volume. Since the  $k^3$  term in the integral heavily weighs on the integrand close to  $k = k_F$ , it follows from the above equation that the temperature dependence of the resistivity is primarily determined by  $s(k = 2k_F)$ .

This is more obvious from the Fig. 4.1. The figure shows the structure factor at a temperature  $T_1$  plotted as function of the  $k$  vector. Quantitatively this may be obtained from the X-ray diffraction pattern using the formula  $k = 2\pi \sin(\theta/\lambda)$ , where  $2\theta$  is the Bragg angle corresponding to the structure factor  $s(k)$ . For our present purposes we need to consider only the region around  $k_p$  the major peak in  $s(k)$ . As the temperature is increased to say  $T_2$ , this peak broadens and all the values near  $k_p$  are reduced. For an alloy with  $2k_F$  in the vicinity of  $k_p$  then a negative TCR is expected. On the other hand if  $2k_F$  is far away from  $k_p$ , all the values of the interference function increase, and so a positive TCR is predicted. Thus, for example, alloying a monovalent element with a multivalent element should produce a positive TCR for electron concentrations less than 1.5, and a negative TCR for 1.5 to 2 effective conduction electrons per ion. This picture is quite similar to the case of crystals, where monovalent elements are expected to be metals and divalent elements are expected to be insulators. Of course divalent elements in the crystalline form are

## Chapter 4

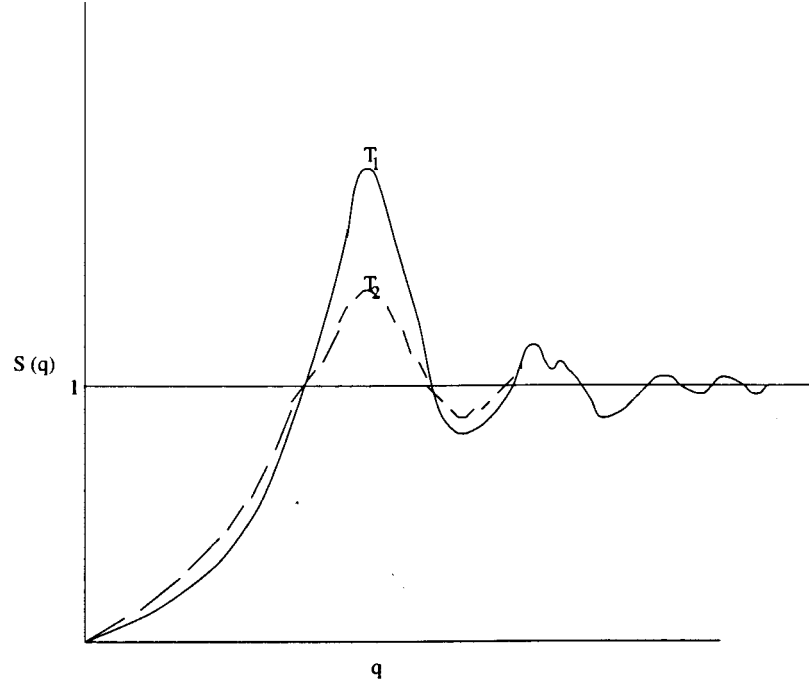


Figure 4.1: The Structure factor of a glass as a function of the scattering wave-vector  $k$  at two temperatures  $T_1$  and  $T_2$

actually metals and not insulators because of the overlap of bands. The electrons in the divalent elements completely fill up the first Brillouin zone and hence they are Bragg reflected by the zone boundary. Hence divalent elements are expected to be insulators with a negative TCR. Similarly in the case of metallic glasses made of divalent elements, electrons are filled up to  $k$  values corresponding to  $k_p$  and hence the Bragg reflection is more in this case. Hence such metallic glasses have a higher resistivity and a negative TCR.

In the case of metallic glasses containing transition elements, the expression for the resistivity is slightly modified to [5]:

$$\rho \sim \frac{30\pi^3 \hbar^3}{me^2 k_F^2 E_F \Omega} \sin^2[\eta_2(E_F)] S_T(2k_F) \quad (4.2)$$

Here  $\eta_2(E_F)$  is the d-partial-wave phase shift describing the scattering of the conduction electrons by the ion cores which carry a muffin-tin potential centered on each ion position. Here the integral in Eq. 4.1 has been approximated by its value at  $k_p$ .

To calculate the TCR using this model, we require the temperature dependence

of the structure factor. Several calculations are available within the framework of the diffraction model, but the one used in the present work yields [6],

$$S_T(k) \simeq 1 + [S_E(k) - 1]e^{-2W_k(T)} \quad (4.3)$$

Where  $S_E(k)$  is the equilibrium structure factor and  $e^{-2W_k(T)}$  is the Debye Waller factor with  $W_k(T)$  in the Debye approximation, given by [7]

$$W_k(T) = W_k(0) + 4W_k(0) \left[ \frac{T}{\theta_D} \right]^2 \int_0^{\theta_D/T} \frac{z dz}{e^z - 1} \quad (4.4)$$

Where

$$W_k(0) = 3\hbar^2 k^2 / 8Mk_B\theta_D \quad (4.5)$$

$M$  is the atomic mass.

With the aid of Eq. 4.2 and Eq. 4.3, the resistivity as a function of temperature can be expressed as:

$$\begin{aligned} \rho_{str}(T) &= \frac{30\pi^3 \hbar^3}{me^2 k_F^2 E_F \Omega} \sin^2[\eta_2(E_F)] \\ &\times \left[ 1 + [S_o(2k_F) - 1]e^{2[W_{2k_F}(T) - W_{2k_F}(0)]} \right] \end{aligned} \quad (4.6)$$

The temperature coefficient of resistivity can be calculated from the above equation

$$\alpha = \frac{1}{\rho} \frac{d\rho}{dT} = 2 \left[ \frac{1 - S_T(2k_F)}{S_T(2k_F)} \right] \frac{dW(T)}{dT} \quad (4.7)$$

For  $T \geq \theta_D$   $W(T)$  is given by [6]

$$W(T) \simeq 4W(0) \left[ \frac{T}{\theta_D} \right] \quad (4.8)$$

Therefore under this approximation,  $a$  is given by:

$$\alpha = 8W(0) \left[ \frac{T}{\theta_D} \right] \left[ \frac{1 - S_T(2k_F)}{S_T(2k_f)} \right] \quad (4.9)$$

This equation demonstrates that  $a$  is negative if  $S_T(2k_F) > 1$  and positive if  $S_T(2k_F) < 1$ . Alternatively, a negative  $a$  is expected only when  $2k_F$  lies in the vicinity of  $k_p$ , the  $k$  value corresponding to the first peak of  $S(k)$ , otherwise a positive  $a$  is expected.

Recently, the applicability of Ziman's theory to metallic glasses has been called into question, especially in cases, where the mean-free path is of the order of the inter-atomic spacing. Experimental results [8] for some glasses show that the decrease of resistivity with temperature is much stronger than that of the Debye-Waller factor for the main peak in the structure factor, which is difficult to account for in the diffraction model.

Even in certain low-resistivity Mg-Zn glasses, which have a long mean free path, a violation of the Mooij correlation has been detected [9]. These low resistivity systems show a negative TCR which violates the Mooij correlation. While inclusion of multiple scattering effects may influence the temperature dependence of resistivity, there is now considerable experimental and theoretical evidence that incipient localization is likely to play a major role in causing the Mooij correlation [10]. Despite these doubts, in the present work the experimental data have been analyzed in terms of the Ziman's theory as it is simple and easy to apply. Any shortcomings of the theory will be exposed in the analysis of the experimental data

### 4.3 AC Resistivity studies on Metallic glasses

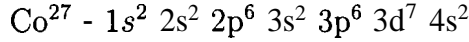
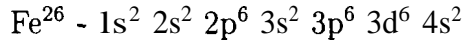
The AC resistivity technique was used for the determination of the resistivity of metallic glasses. The first glass chosen for this study was  $Fe_{73.5}Cu_1Nb_3Si_{13.5}B_9$ . The specific heat study of this glass showed a unique step-like behaviour at  $T_c$ . Also the Curie temperature for this glass was known. This was the motivation for doing the AC resistivity study on this glass. The other glasses studied were  $Co_{65}Fe_5Mo_2B_{12}Si_{16}$  and  $Fe_{70}Co_{15}B_{15}$ .

The resistivity studies were carried out using the four-probe ac resistivity technique described in chapter 2. High pressure studies were carried out in the piston-cylinder apparatus using the High-Temperature High-Pressure cell. For resistivity studies, the metallic glass is taken in the form of a thin foil of dimensions  $40 \mu\text{m} \times 10\text{mm} \times 2\text{mm}$

#### 4.3.1 Results and Discussion

Resistivity studies were performed on Iron-rich and Cobalt-rich metallic glasses. While Iron-rich metallic glasses show a positive temperature coefficient of resistance, Cobalt-rich glasses show a negative temperature coefficient of resistance. We can attribute the difference in the TCR for the two glasses to differing electron concentrations in them.

Iron has 26 electrons which are distributed among the different orbitals in the following manner:



However the electronic configuration given above is valid only in the case of an isolated atom. In a solid there are usually non-integral number of electrons in the s and d orbitals due to s-d hybridization. s-d hybridization is the reason for the magnetic moment/per atom being a non-integral number of Bohr magnetons. According to data from magnetization measurements [11], the magnetic moment/Iron atom at 0 K is 2.2 Bohr magnetons ( $\mu_B$ ), while the magnetic moment of Cobalt is  $1.7 \mu_B$ . From this it can be seen that the number of s-electrons is around 0.2/atom in the case of Iron and 0.7 in the case of Cobalt. The s-electrons are the ones which make the major contribution to the electrical conductivity.

The effective number of charge carriers per atom is calculated by taking into account the number of free electrons contributed by the other elements in the metallic glass. Assuming that each Silicon atom contributes 4 electrons, Boron 3, Copper 1, Niobium 2 and Molybdenum 2, the number of free electrons/atom per atom turns out to be 1.027 in the case of  $\text{Fe}_{73.5}\text{Cu}_1\text{Nb}_3\text{B}_9\text{Si}_{13.5}$  and 1.5 in the case of  $\text{Co}_{65}\text{Fe}_5\text{Mo}_2\text{B}_{12}\text{Si}_{16}$ . Hence  $2k_F$  will be nearer to  $k_p$  in the case of  $\text{Co}_{65}\text{Fe}_5\text{Mo}_2\text{B}_{12}\text{Si}_{16}$ . Therefore a negative TCR is to be expected for this glass on the basis of Ziman's theory.

#### **Resistivity of $\text{Co}_{65}\text{Fe}_5\text{Mo}_2\text{B}_{12}\text{Si}_{16}$ :**

Fig. 4.2 shows the resistance of  $\text{Co}_{65}\text{Fe}_5\text{Mo}_2\text{B}_{12}\text{Si}_{16}$  as a function of temperature. The resistivity runs were performed at a rate of  $5^\circ \text{C}/\text{min}$ . The sample was cooled once the temperature reached  $200^\circ \text{C}$  and then cooled back to room temperature. This glass has a Curie temperature of  $160^\circ \text{C}$ . The resistivity does not seem to show any change near  $T_c$ . The resistivity runs were repeated after the sample had cooled to room temperature. It is seen from the figure that the resistance of the sample increases with successive heating and cooling runs. Such a phenomenon has been observed by earlier workers and has been explained on the basis of Ziman's theory. Since a metallic glass is in a metastable condition, its configuration could change on repeated heating and cooling. One of the changes observed on repeated heating and cooling is that the first peak in the diffraction pattern becomes more and more sharper. Due to this, if  $2k_F$  is near the peak in the structure factor, then one would expect the resistance to increase, as in the present case. If  $2k_F$  lies far

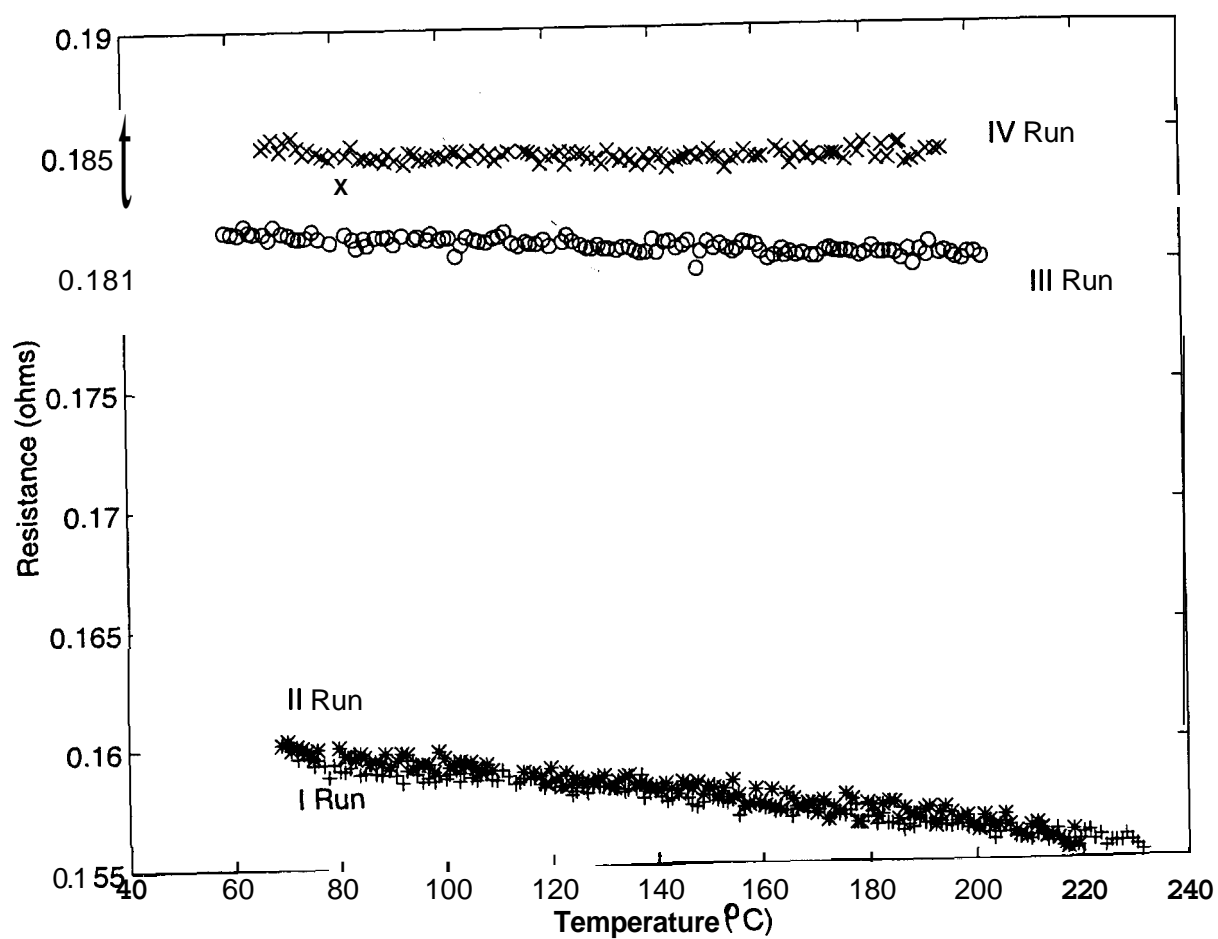


Figure 4.2: Resistance of  $Co_{65}Fe_5Mo_2B_{12}Si_{16}$  as a function of temperature

from  $k_{\parallel}$ , then one would expect a decrease in the resistance with successive heating runs. Another feature which is also noticeable from the figure is that the TCR also seems to change with the heat treatment.

To explain this, we recall the expression for the temperature coefficient of resistance:

$$\alpha = 8W(0) \left[ \frac{T}{\theta_D} \right] \left[ \frac{1 - S_T(2k_F)}{S_T(2k_f)} \right] \quad (4.10)$$

From this equation, we notice that there are two contributions to the TCR. If  $S_T(2k_F)$  increases with annealing, as one has mentioned above, then the TCR should decrease in magnitude. There is usually another effect which adds to this effect. It is well known that repeated heat treatment of the glass leads to an increase in its density. Since  $\alpha \propto \frac{1}{\rho^2}$ , and  $\theta_D$ , the Debye temperature increases with density, this effect leads to an additional increase in the TCR.

### **Resistivity Results for $Fe_{73.5}Cu_1Nb_3B_9Si_{13.5}$**

#### **Effects of heat treatment:**

As in the case of  $Co_{65}Fe_5Mo_2B_{12}Si_{16}$ , it is seen that the resistance shows a history-dependent behaviour. The resistance decreases with each successive run. This is in accordance with Ziman's theory as this glass has a positive temperature coefficient. The first run shows a large decrease in the resistance. After a few runs the resistivity (at a particular temperature) seems to settle into an equilibrium value, which does not change much with successive runs.

The data for 2<sup>nd</sup>, 3<sup>rd</sup> and 4<sup>th</sup> runs could be fitted to a quadratic equation of the form

$$r = r_o + r_1T + r_2T^2 \quad (4.11)$$

$\alpha$  at 300° C is **8.6** x 10<sup>-5</sup> for the second run and **6.7** x 10<sup>-5</sup> for the third run.  $\alpha$  is given by

$$a = r_1/r(T) \quad (4.12)$$

The coefficient  $r_2$  is of the order of 10<sup>-8</sup>. This value of  $r_2$  is close to the value obtained by Kaul et al [12]. According to Kaul et al the  $T^2$  contribution to the resistivity comes from the magnetic contribution to the electron scattering. The change in the magnetic contribution to the resistivity above  $T_c$  is not seen in the present experimental data, except at 1 bar and at 20 kbar. The sensitivity of the

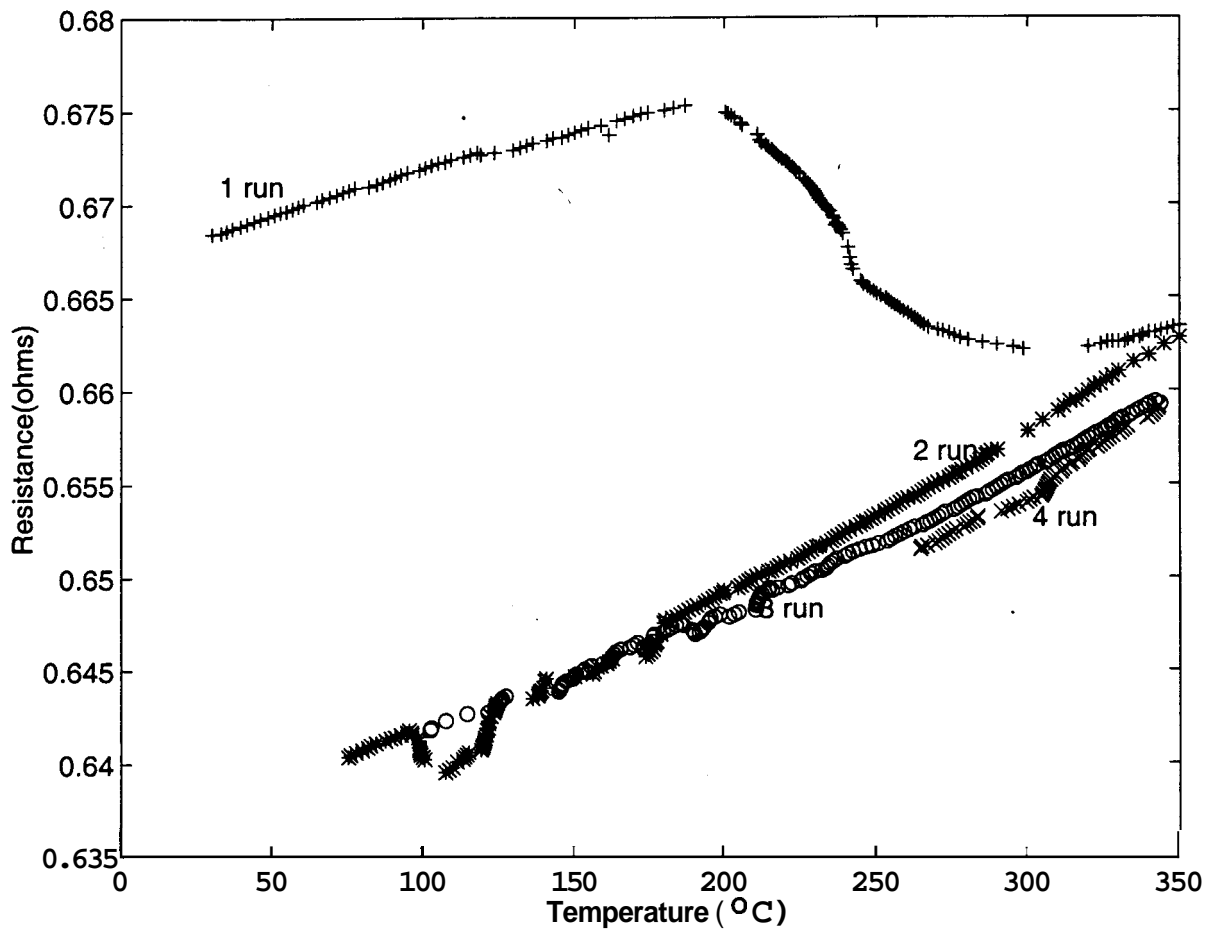


Figure 4.3: Resistance of  $Fe_{73.5}Cu_1Nb_3B_9Si_{13.5}$  as a function of temperature

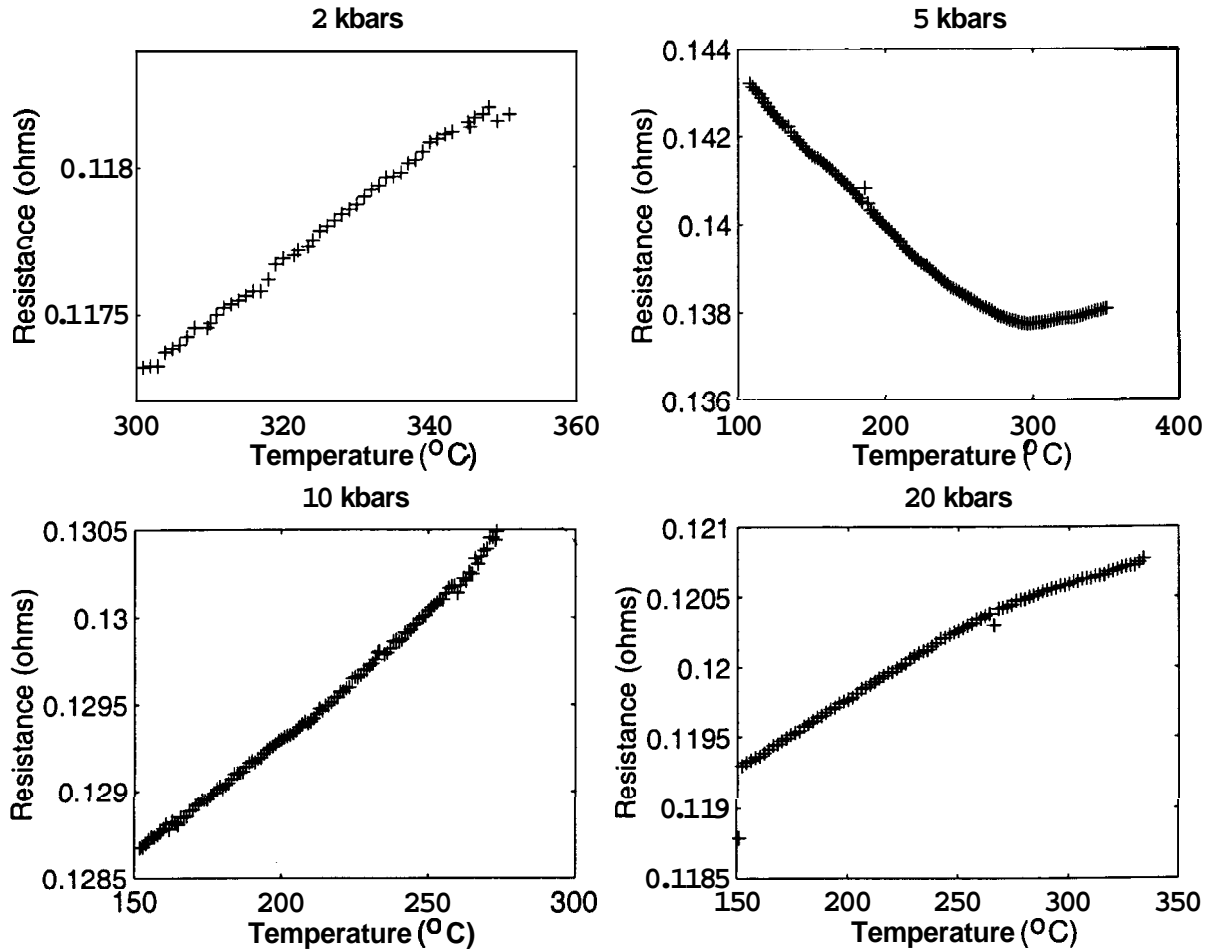


Figure 4.4: Resistance of  $Fe_{73.5}Cu_1Nb_3B_9Si_{13.5}$  as a function of temperature at different pressures

experimental arrangement used here is 1 in 1000, whereas kaul et al have obtained a resolution of 1 in  $10^6$  and hence could detect the change in resistivity at  $T_c$ .

#### 4.3.2 High pressure resistivity studies on $Fe_{73.5}Cu_1Nb_3B_9Si_{13.5}$

High pressure resistivity studies were conducted on  $Fe_{73.5}Cu_1Nb_3B_9Si_{13.5}$  using the high-temperature high-pressure cell described in section 4.3. The resistance is shown in Fig. 4.4 as a function of temperature at different pressures. The resistance of the metallic glasses at these pressures could also be fitted to a quadratic equation similar to Eq. 4.11. The values of  $\alpha$  and  $r_2$  obtained from this fit are tabulated here:

The resistivity seems to have a negative TCR when the pressure is 5 kbar.

## Chapter 4

Table 4.1: Pressure dependence of  $a$  and the coefficient of the  $T^2$  term

Pressure (kbar)	$\alpha$ ( $^{\circ}\text{C}$ )	$r_2$
1 bar (2 <sup>nd</sup> run)	$8.62 \times 10^{-5}$	$7.10 \times 10^{-8}$
1 bar (3 <sup>rd</sup> run)	$6.70 \times 10^{-5}$	$6.48 \times 10^{-8}$
2	$1.62 \times 10^{-4}$	-
10	$2.82 \times 10^{-5}$	$2.51 \times 10^{-8}$
15	$1.74 \times 10^{-5}$	$1.33 \times 10^{-8}$

However this is true only for the first run after the sample is pressurized. Subsequent runs show only a positive TCR. This is true of the resistivity at 10 and 15 kbar also. The first run after pressurization shows a negative TCR, while subsequent runs show only a positive TCR.

This can be explained by assuming that there is a change in the value of  $S_T(2k_F)$ . This assumption is supported by the fact that the value of the resistance has increased when the sample is pressurized from 2 kbar to 5 kbar. It has to be noted that just a decrease in the nearest neighbour distance due to pressurization does not lead to a relative shift between the positions of  $2k_F$  and  $k_p$ . An increase in density shifts the position of  $k_p$  as  $k_p \propto d^{1/3}$  (where  $d$  is the density of the glass). However since  $k_F$  is also proportional to  $d^{1/3}$ , there is no relative shift between  $2k_F$  and  $k_p$  and hence the resistivity remains unchanged. However increasing pressure might also lead to an increase in the number of nearest neighbours for each atom. Since the area under the first peak of  $S(k)$  is proportional to the number of nearest neighbour atoms, the value of  $S(2k_F)$  might increase, thus leading to an increase in the resistance and possibly changing the sign of the TCR if  $S(2k_F)$  becomes greater than 1. When the sample is subsequently heated and cooled, the peaks might sharpen, and the value of  $S(2k_F)$  reverts back to its old value. Hence the TCR becomes positive once again. This brings out an important difference in the response of crystalline and non-crystalline systems to the application of pressure. While in crystalline systems, the application of pressure only leads to a monotonic decrease in the lattice constant, in the case of glassy systems and liquids, it could lead to a change in the number of nearest neighbours in addition to a decrease in the inter-atomic distance. From the values of  $a$  tabulated, no systematic variation of  $a$  with pressure is apparent.

## Chapter 4

### 4.4 Thermopower of Metallic Glasses

#### 4.4.1 TEP Measuring System

For measuring the TEP of the metallic glass, the sample is placed along the axis of the high temperature cell described earlier. The arrangement of the sample in the high temperature cell is identical to the cell arrangement for the resistivity studies, except for the fact that the sample is placed vertically in order to take advantage of the natural temperature gradient which exists in the furnace. The TEP is measured using the procedure described in section. 2.5.

#### 4.4.2 Thermopower of metallic glasses on the basis of Ziman's theory

The absolute TEP of the metallic glasses may be deduced from Mott's formula:

$$S = \frac{\pi^2 k^2 T}{3|e|\xi_F} \xi \quad (4.13)$$

Where  $\xi$  is given by:

$$\xi = -\xi_F \left[ \frac{d \ln \rho(\xi)}{d\xi} \right]_{\xi=\xi_F} \quad (4.14)$$

The TEP for metallic glasses can be deduced from the basic formula for the resistivity by differentiating with respect to the position of the Fermi level.

This gives

$$\xi = 3 - 2q - \frac{1}{2}r \quad (4.15)$$

Where  $q$  is due to the variation of the upper limit of integration in Eq. 4.1.

$$q = \frac{|u(2K_F)|^2 S(2K_F)}{\langle |u(K)|^2 S(K) K^3 \rangle} \quad (4.16)$$

$r$  comes from variation of the pseudopotential.

$$r = \frac{2\xi_F \langle (\partial |u(K)|^2 / \partial \xi_F) S(K) K^3 \rangle}{\langle |u(K)|^2 S(K) K^3 \rangle} \quad (4.17)$$

Using the above equation it is seen that for metallic glasses which have a high value of  $S(2K_F)$ ,  $2q > 3$  and hence the thermopower is positive. The same condition leads to a negative temperature coefficient of resistance as noted in the last section. If  $2q < 3$ , then the thermopower is negative, while the TCR will be positive. This

correlation between the sign of the thermopower and the sign of TCR was experimentally verified by Nagel [17]. However in the case of magnetic glasses like the present system this correlation is not found to hold good. Also the Ziman's theory can give only a linear dependence on temperature for TEP. The experimental results to be discussed in the next section show that the thermopower of most metallic glasses containing transition elements have a non-linear dependence on temperature. This forces us to look for alternative explanations for explaining the TEP results.

#### 4.4.3 Thermopower of $Fe_{73.5}Cu_1Nb_3B_9Si_{13.5}$

The Thermopower results for  $Fe_{73.5}Cu_1Nb_3B_9Si_{13.5}$  are shown in Fig. 4.5. The thermopower, unlike the electrical resistivity, does not seem to be history dependent. This is because the thermopower is mainly dependent on the electronic structure of the material rather than the structural configuration. So even if the resistivity of the glass changes by heat treatment, its thermopower, which is related to the derivative of the resistivity will remain unchanged. The thermopower was determined by the differential method discussed earlier using a heating rate of  $5^\circ C/min$ . The most prominent feature of the TEP curves is a minimum around  $130^\circ C$  to  $140^\circ C$ . This feature seems to occur at the same temperature irrespective of the pressure. Such a minimum has been observed by earlier workers, but it is mentioned in the literature that such a minimum occurs at around  $T_c/2$ . For the present metallic glass,  $T_c$  shifts by about  $7^\circ C$  for an increase of 1 kbar pressure. However the minimum does not shift with pressure, indicating a non-magnetic origin for the minimum. The Curie point transition in this glass manifests as a change of slope in the TEP vs temperature curve. The shift in  $T_c$  with pressure can be clearly seen in the figure. The Curie point transition is seen much more clearly in the specific heat measurements, which are described in the next chapter. The minimum in the TEP also occurs in the case of crystalline Iron. Since Iron is the predominant element in this glass one would expect the behaviour of Iron to dominate over the other components.

#### 4.4.4 Discussion of Results

The minimum in the thermopower does not shift with the application of pressure. This seems to hint that the minimum may not be of magnetic origin. Instead it has to be explained from very general considerations of the band-structure of Iron.

The TEP results are usually interpreted in terms of the Mott's formula for diffusion thermopower.

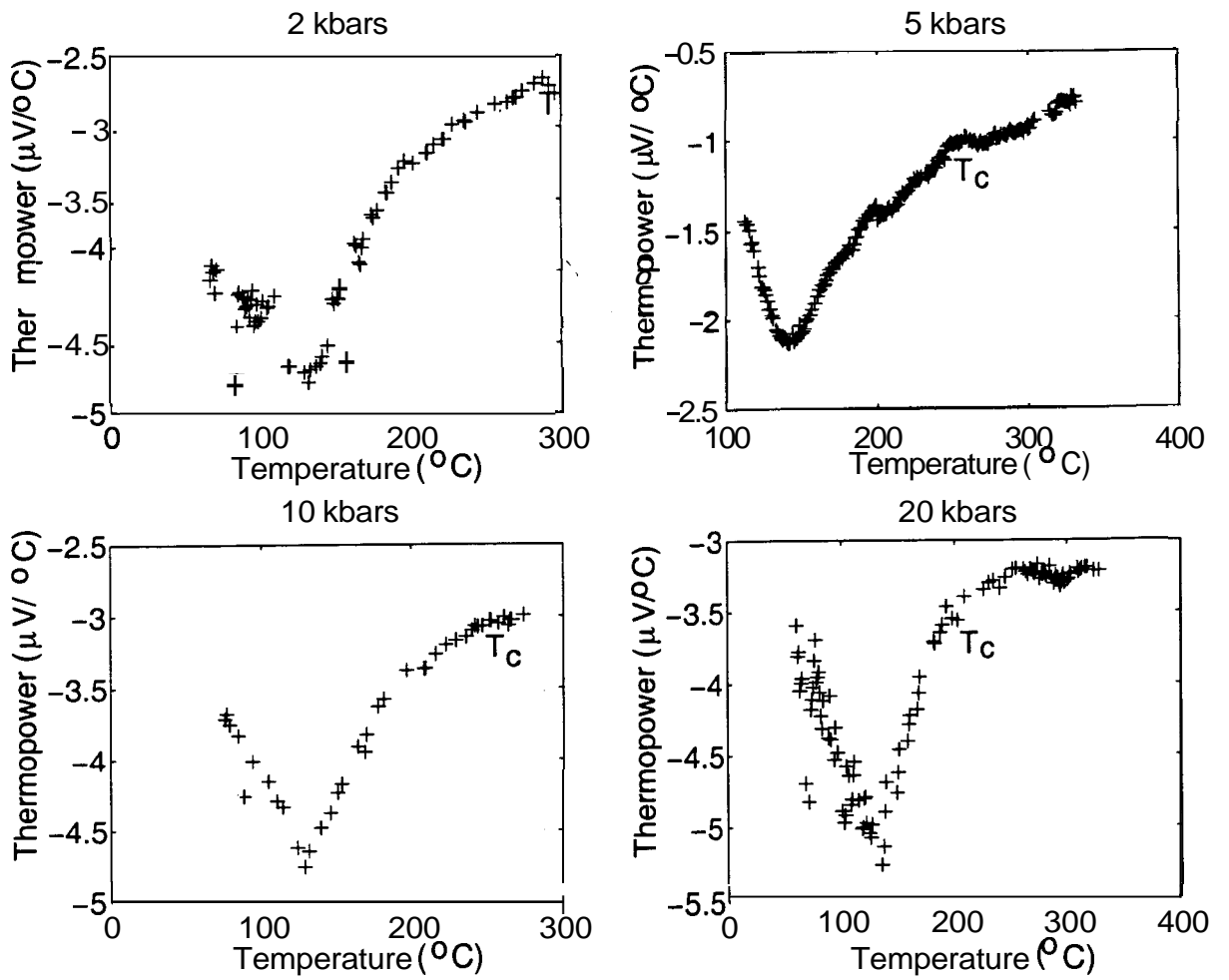


Figure 4.5: Thermopower of  $\text{Fe}_{73.5}\text{Cu}_1\text{Nb}_3\text{B}_9\text{Si}_{13.5}$  as a function of temperature at different pressures

Chapter 4

$$S_{diff} = \left[ \frac{\pi^2 k^2 T}{3e} \frac{d \ln a}{dE} \right]_{E=E_F} \quad (4.18)$$

Where  $a$  is the conductivity and  $e$  is the electronic conductivity. Therefore the thermopower is given by the derivative of the electrical conductivity with respect to energy evaluated at the Fermi energy.

The electrical conductivity is given by Drude's formula:

$$\sigma = \frac{ne^2\tau}{m} \quad (4.19)$$

This equation is based on the free-electron approximation. For transition metals, it is more appropriate to write this formula in the following form:

$$\sigma(E_F) = \frac{2}{3} e^2 v_s^2 \tau_s (N_s(E))_{E=E_F} \quad (4.20)$$

Where  $\tau$  is the relaxation time and  $N_s$  is the density of states of s-electrons. In the case of transition metals the predominant mechanism for scattering is the scattering of the s electrons responsible for conduction into the less-mobile d states. The relaxation time will be less, if there are more number of d-states available for the scattered electrons. Therefore

$$\tau = \frac{1}{N_d} \quad (4.21)$$

Where  $N_d$  is the density of d-states.

Thus,

$$\sigma(E_F) = A v_s^2 \left[ \frac{N_s(E)}{N_d(E)} \right]_{E=E_F} \quad (4.22)$$

where  $A$  is a constant with respect to energy

In the case of transition metals like Iron it is well known density of states has the following form [18]:

$$N_d = N_o (E_o - E)^{1/2} \quad (4.23)$$

Where  $E_o$  is the energy corresponding to the top of the d-band. Now using Eq. 4.18, Eq. 4.20 and Eq. 4.21, we get

$$S = \left[ \frac{\pi^2 k^2 T}{3e} \left( \frac{3}{2E_F} \frac{d \ln N_d}{dE} \right) \right]_{E=E_F} \quad (4.24)$$

Differentiating Eq. 4.23 we get

$$\frac{d \ln N_d}{dE} = \frac{-1}{2(E_o - E_F)} \quad (4.25)$$

If we substitute this result in Eq. 4.18, we would get a thermopower which has a negative sign and a linear temperature dependence. Also  $dS/dT$  would have a negative sign, due to the sign of the electronic charge. This is in contrast to experimental results which show that  $dS/dT$  is positive beyond 150° C. To explain these facts we would have to take into account the fact that in a ferromagnetic system, the bands are split into spin-up and spin-down bands, due to the magnetic interaction. Since there are more electrons in the spin-up band compared to the spin-down band the spin-up band will be filled to a greater extent than the spin-down band (Fig. 4.6b). Since the chemical potential (Fermi energy) of the two-bands, should be the same, the spin-up band is pushed down with respect to the spin-down band as shown in Fig. 4.6. Due to this, the number of available d states at  $E_F$  is more in the case of the spin-down band than the spin-up band. Hence the electrons will be predominantly scattered into the spin-down band.

Mott, [18] has calculated the diffusion thermopower using such a model. He assumes that the spins are not flipped during the scattering. The final result of Mott's analysis is:

$$S = const.T \left[ \frac{1}{(1-M)^{1/3}} \frac{\alpha + (1+M)^{1/3}}{\alpha + (1-M)^{1/3}} + \frac{1}{(1+M)^{1/3}} \frac{\alpha + (1-M)^{1/3}}{\alpha + (1+M)^{1/3}} \right] \div [2\alpha + (1+M)^{1/3} + (1-M)^{1/3}] \quad (4.26)$$

Here  $M$  is the magnetization and  $a$  is the ration of s-s scattering events to s-d scattering events, given by

$$\alpha = \frac{N_s}{N_d} \quad (4.27)$$

$const$  is given by

$$const = \frac{\pi^2 k^2}{3e} \quad (4.28)$$

Mott has shown that the prediction of this formula is roughly obeyed for the case of transition metals like Nickel. The experimental results for  $Fe_{73.5}Cu_1Nb_3B_9Si_{13.5}$  are qualitatively similar to the predictions of this formula. This model predicts that  $dS/dT$  has a positive sign below  $T_c$  and a negative sign above  $T_c$ . It predicts a change in the sign of  $ds/dT$  at  $T_c$ , though the sign of  $S$  is always negative. In the case of  $Fe_{73.5}Cu_1Nb_3B_9Si_{13.5}$ , the change of sign in  $dS/dT$  is not very obvious. In contrast to this, the thermopower of crystalline Iron, Nickel and Cobalt clearly show this change in slope. This can be understood qualitatively from Eq. 4.27. Above  $T_c$ , since  $M = 0$ , Eq. 4.27 simplifies to

Chapter 4

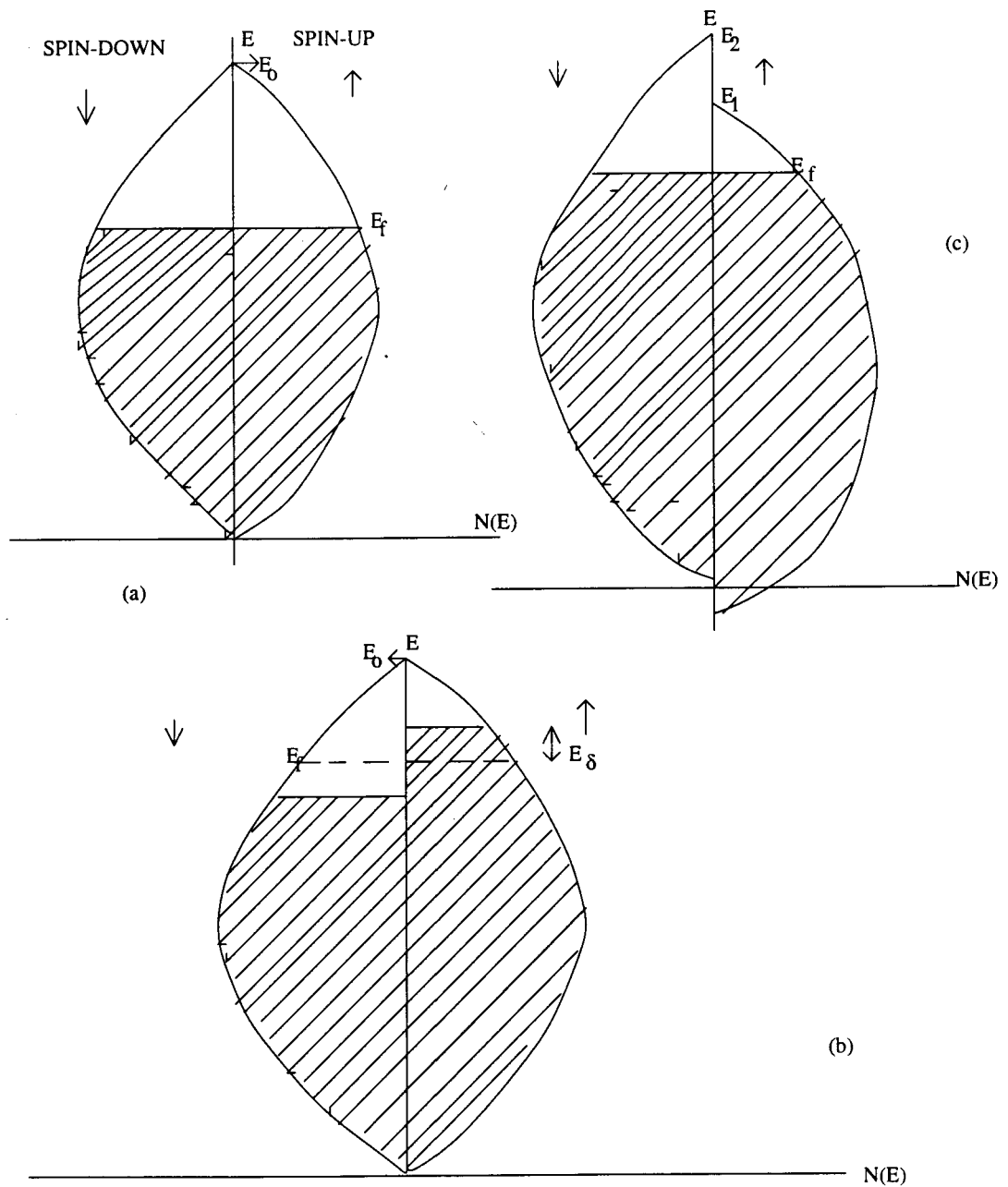


Figure 4.6: Density of d-electron states in a transition metal. a) Paramagnetic state b) and c) Ferromagnetic state

## Chapter 4

$$S = \frac{\pi^2 k^2 T}{3e} \frac{1}{\alpha + 1} \quad (4.29)$$

In the case of metallic glasses as compared to elemental Iron, the d-band will be filled up more due to charge transfer from the metalloids. This means that  $a$  will have a higher value when compared to Iron. This in turn means that  $S$  and  $dS/dT$  will have a lower magnitude in the case of the glasses. This result is reflected in the data for  $Fe_{73.5}Cu_1Nb_3B_9Si_{13.5}$ .

The thermopower at a particular temperature reduces with pressure. This is in agreement with the present theory. When the pressure is increased, the Fermi energy,  $E_F$ , increases due to the increase in electron concentration, however  $(E_o - E_F)$  remains unchanged. So the combined effect of this is to reduce the thermopower at a particular temperature.

The insensitiveness of  $T_{min}$  to pressure is somewhat surprising. It might be due to the fact that while the Debye temperature increases with pressure the Curie temperature decreases with pressure. Therefore while one would expect the magnon drag at a particular temperature to reduce, the phonon drag might increase, hence the combined effect of the phonon and the magnon drag remains unchanged. Of course there is a small decrease in the diffusion thermopower with increase of pressure.

### 4.5 Conclusions

The electrical transport properties of metallic glasses containing transition elements were studied. While the resistivity results showed features characteristic of the amorphous state, the thermopower seems to be independent of the glassy nature and is not very different from that of the crystalline state. The resistivity shows some history dependent effects, which have been related to structural changes in the glass. The thermopower does not show any history-dependent effects. The thermopower does not follow the predictions of Ziman's theory below  $T_c$ .

## References

- [1] K.V.Rao, in Amorphous metallic alloys, edited by F.E. Luborsky (Butterworths, London,1983), p.401
- [2] J.H.Mooij, Phys.Stat.Solidi, **A17**, 521 (1973)
- [3] P.J.Cote and L.V.Meisel, Top.Appl.Phys., 46, 141 (1981)
- [4] J.M. Ziman, Phil.Mag, 6, 1014 (1961)
- [5] R.Evans,D.A. Greenwood, and P.Lloyd, Phys.Lett.**35A**, 57 (1971)
- [6] S.R.Nagel, Phys.Rev.**B 16**, 1694 (1977)
- [7] J.M.Ziman, Principles of the theory of Solids, Cambridge University Press, 1972
- [8] K.D.D.Rathnayaka, A.B.Kaiser and H.J.Trodahl, Phys.Rev.B, 33, 889 (1986);  
K.D.D.Rathnayaka, H.J.Trodahl and A.B.Kaiser, Solid State Commun., 57,  
207 (1986)
- [9] J.Hafner, J.Non-Cryst.Solids, **69**, 325 (1985)
- [10] S.M.Girvin and M.Jonson, Phys.Rev.B, 22, 3583 (1980); Y.Imry,  
Phys.Rev.Lett., 44, 469 (1980); M.Kaveh and N.F.Mott, J.Phys.C, 15,  
L 707 (1982); M.A.Howson, J.Phys.F, 14, L25 (1984); M.A.Howson and  
D.Grieg, ibid, 16, 981 (1986)
- [11] N.F.Mott, Adv.Phys.,**13**, 325 (1964)
- [12] S.N.Kaul, W.Kettler and M.Rosenberg, Phys.Rev.B, 33, 4987 (1986)
- [13] V.Shubha and T.G.Ramesh, High temp.High Press., 18,311 (1986)
- [14] Reshamwala A.S and Ramesh T.G, J.Phys.E (Sci.Instrum), 7, 133 (1974)
- [15] R.D. Barnard in Thermoelectricity in Metals and Alloys, Taylor and Francis LTD, 1972

## Chapter 4

[16] V.Shubha and T.G.Ramesh High Temp. High Press., 9 461 (1977)

[17] S.R.Nagel, Phys.Rev.Lett., 41, 990 (1978)

[18] N.F.Mott, Proc.Roy.Soc.Ser. **A156**, 368 (1936)

## Chapter 5

# Pressure dependence of Curie Temperature in Metallic Glasses

### 5.1 Introduction

There are two theoretical approaches to metallic magnetism, namely the localized and the itinerant electron approaches. The former is concerned with localized magnetic moments in direct exchange interaction. In its simplest form it applies to non-metallic magnets. For metals and alloys, the itinerant electron model is more appropriate. In applying this model to amorphous alloys many 'localized' features must also be considered. Unfortunately, the itinerant electron model is difficult to apply even to the pure metals such as Iron and Nickel. Hence the application to complicated alloys, which the amorphous magnets certainly are, is more difficult.

High Pressure studies on metallic glasses can help us in building realistic models for the magnetism in these glasses. The itinerant and localized models give differing predictions for the pressure dependence of the Curie temperature. Hence measurement of the Curie temperature as a function of pressure can help in identifying the most appropriate model to describe amorphous magnetism.

The magnetism in metallic glasses is complicated by the fact that in addition to positional disorder, one also has to contend with chemical disorder due to the presence of the metalloids like Boron and Silicon. The presence of the metalloids leads to charge transfer between these two species of atoms (e.g,  $B \rightarrow Fe$ ). This transfer is, however, not a simple movement of electrons in space but is related to the hybridization of the d electrons on the transition metal atoms with s-p electrons on the metalloids.

A paramagnetic band calculation [1] on crystalline  $Fe_3Si$  shows that a 3d band containing tens states per transition metal atom can be regarded as being gradually

filled as the concentration of the metalloids increases. These states are not localized on the transition metal atoms but their wave functions also have a considerable weight on the metalloids. This concept replaces that of spatial charge transfer but has the same effect.

In the itinerant electron model, the interaction between two electrons on the same lattice site, is of the form:

$$I_o = \int \frac{e^2}{r_{12}} |\phi(\mathbf{r}_1)|^2 |\phi(\mathbf{r}_2)|^2 d\mathbf{r}_1 d\mathbf{r}_2 \quad (5.1)$$

Where  $r_1$  and  $r_2$  are the position co-ordinates of the electrons and  $r_{12}$  is the separation between them.

This interaction is by itself too large, since it is based on an inadequate approximation (Hartree-Fock) to this problem. However, an improvement to include correlation effects, due to Kanamori [1] and Hubbard [2], leads to a smaller value  $I$ , given approximately by

$$I = \frac{I_o}{(1 + \gamma I_o/W)} \quad (5.2)$$

Where  $\gamma$  is a constant of order unity and  $W$  the energy band width. This formula has been used to discuss the magnetovolume anomalies of many amorphous ferromagnets, since the bandwidth  $W$  of the 3d electrons varies approximately as  $R_1^{-5}$  [3].

Knowing the bandwidth and the density of states at the Fermi level, one can use Stoner's criterion for ferromagnetism [5]

$$\bar{I} = IN(E_F) > 1 \quad (5.3)$$

Therefore there are two competing effects which determine the Curie temperature.  $I$  increases with pressure (since the bandwidth increases under pressure) thus favouring the condition for ferromagnetism, but at the same time the density of states.  $N(E_F)$  will decrease with increase in pressure which has the exactly opposite effect. The sign of  $dT_c/dP$  is determined by the factor which dominates among these two.

According to the work of Chien and Unruh [4] there are ranges of metalloid content where the saturation magnetization  $M(0)$  and  $T_c$  vary in the same sense and others where this sense is opposite. For weak ferromagnets ( $\bar{I} - 1 \ll 1$ ) a variation in the same sense is expected, i.e,

$$M(0) \sim T_c \sim (\bar{I} - 1)^{1/2} \quad (5.4)$$

The pressure dependence of  $T_c$  can be calculated on the basis of this relation, which is more explicitly of the form,

$$T_c^2 = T_F^2(\bar{I} - 1) \quad (5.5)$$

Here  $T_F$  is the so-called 'effective degeneracy temperature' given by :

$$T_F^{-2} = \frac{1}{6}\pi^2 k^2 \left[ \frac{N''}{N} - \left( \frac{N'}{N} \right)^2 \right]_{E=E_F} \quad (5.6)$$

in terms of the derivatives of the density of states curve. For ferromagnetic alloys  $T_F$  varies about a mean value about  $10^3$  K.

On the basis of this theory, discussed in detail by Wohlfarth [5] it follows that:

$$T_c(P) = T_c(0)(1 - P/P_c)^{1/2} \quad (5.7)$$

and

$$dT_c/dP = \frac{5}{3}\kappa T_c - \alpha/T_c \quad (5.8)$$

Where

$$P_c = T_c^2(0)/2\alpha \quad (5.9)$$

is the critical pressure required for the disappearance of ferromagnetism.

and

$$\alpha = \frac{5}{6}\kappa \frac{I}{I_0} T_F^2 \quad (5.10)$$

Where  $\kappa$  is the compressibility.

The first term in Eq. 5.8 is usually small compared with the second and one manifestation of the Invar behaviour, characteristic of these metallic glasses containing Iron, is in fact a large negative pressure derivative of the Curie temperature.

## 5.2 Landau theory for metallic glasses

Wohlfarth has also discussed the ferromagnetic-paramagnetic transition in metallic glasses on the basis of a Landau theory. The Landau free energy is given by:

$$G = \frac{1}{2}AM^2 + \frac{1}{4}BM^4 + \frac{1}{2\kappa}\omega^2 - C\omega M^2 + P\omega \quad (5.11)$$

## Chapter 4

Where for the itinerant electron model.

$$A = -\frac{1}{2\chi_o} \left(1 - \frac{T^2}{T_c^2}\right) \quad (5.12)$$

and

$$B = \frac{1}{2\chi_o M(0)^2} [1 + O(T^2)] \quad (5.13)$$

$$\chi_o = \mu_B^2 N(E_F) / (\bar{I} - 1) \quad (5.14)$$

C is the magnetoelastic coupling constant given by:

$$C = \frac{5}{6} \frac{1}{N(E_F) \mu_B^2} \left[ \frac{1}{2} \frac{I}{I_o} - \frac{T_c^2}{T_F^2} \right] \quad (5.15)$$

Since  $T_c^2 \ll T_F^2$ , C is usually positive.

In the expression for the free energy,  $\kappa$  is the compressibility of the glass,  $w$  the volume strain and  $P$  is the hydrostatic pressure applied on the system. While the terms involving  $M^2$  and  $M^4$  are the usual terms in a Landau free energy, as discussed in chapter 1, the other terms require some explanation. The term  $Pw$  is obviously the work done in applying a pressure  $P$ . This depends on the sign of the volume strain. Hence one more term  $\omega^2/2\kappa$  is added to take into account dissipative forces, which does not depend on the sign of  $w$ . The other term which is a product of  $w$  and  $M^2$  is due to magnetostriction or the coupling between the magnetization and the volume strain.

Minimizing  $G$  with respect to  $\omega$  and substituting the value for  $w$  back into Eq. 5.11 gives:

$$G = \frac{1}{2} A' M^2 + \frac{1}{4} B' M^4 + const. \quad (5.16)$$

Where

$$A' = A + 2\kappa CP \quad (5.17)$$

and

$$B' = B - 2\kappa C^2 \quad (5.18)$$

As seen from the above equations the magnetoelastic coupling seems to affect the free energy. We can calculate the effect of the magnetoelastic coupling on the other thermodynamic quantities like magnetization. Since  $\kappa$ , the compressibility is

always positive and  $C$  is also generally positive as mentioned above, it means that  $A' > A$  and  $B' < B$ . From Eq. 5.11,

$$M = \left( \frac{A'(T_c - T)}{2B'} \right)^{1/2} \quad (5.19)$$

Hence the magnetization at a particular temperature is enhanced by the magnetoelastic coupling.

The Curie temperature is obtained from  $A' = 0$ , i.e.,

$$\frac{dT_c}{dP} = -2\kappa C \chi_o T_c \quad (5.20)$$

Substituting for  $C$  and  $\chi_o$  in the above equation and neglecting the small positive term, we get

$$\frac{dT_c}{dP} = -\frac{\alpha}{T_c} \quad (5.21)$$

In the case of heterogenous alloys, this relation gets modified to:

$$\frac{dT_c}{dP} \sim -T_c \quad (5.22)$$

A more general expression than Eq. 5.21, involves a power of  $T_c$  going as  $-T_c^{-(1/\tau)+1}$ , where  $\tau = 1/2$  if Fermi statistics are used as in Wohlfarth's theory and  $\tau = 3/4$  if Bose statistics are used, as in the theory of T.Moriya [6]. The theory of Moriya deals with spin fluctuations.

Hence an experimental measurement of the pressure dependence of  $T_c$  will help in deciding which model is suitable for a description of the magnetism in these metallic glasses. A distinction between the opposing models can, however, be made on the basis of differing values of  $\tau$ , if the concentration fluctuations which we are present in metallic glasses are small.

Another important feature of the Landau theory formulated by Wohlfarth, is that since the coefficient of the  $M^2$  term is  $T^2 - T_c^2$ , the effect of fluctuations is less. This is seen from Fig. 5.1. The energy cost for a small fluctuation in the order parameter in the case of the present model is much more than the energy cost for the usual  $T - T_c$  term in a Landau theory (Eq. 1.6). The curve for the  $T - T_c$  term (curve B) has almost the same energy for a wider energy range than for curve A (corresponding to the itinerant model)

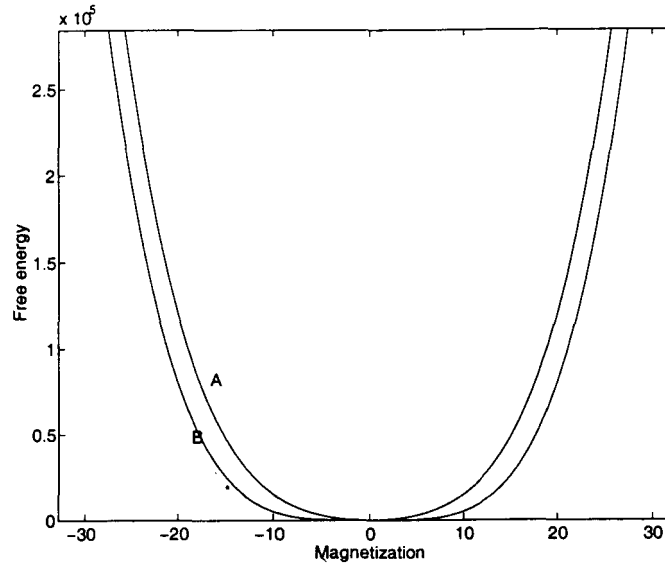


Figure 5.1: The Free energy as a function of the order parameter for a normal Landau theory (curve B) and for the itinerant model (curve A)

---

### 5.3 Predictions of the localized model

There exists another model originally due to Heisenberg, which assumes that the electrons responsible for magnetism in metals are localized at the atomic sites. In this model the magnetic interaction is due to the overlap of the electron clouds on adjacent atoms. The variation of  $T_c$  with pressure, in this model is dependent on the variation of the interaction energy  $J$ . The spatial variation of  $J$  is shown in Fig. 5.2, where  $J$  is plotted against  $r$ , where  $r$  is the ratio of the interatomic distance to the diameter of the unfilled  $d$  shell.

In the localized picture  $T_c$  is directly proportional to  $J$ . The values of  $J$  corresponding to each of the transition elements is shown in the figure. The pressure variation of  $T_c$  in Nickel can be accounted for on the basis of this model also. When Nickel is pressurized, the interatomic distance reduces and since  $J$  increases for smaller values of  $r$  (for Nickel)  $T_c$  increases, which is consistent with observations for Nickel [11].

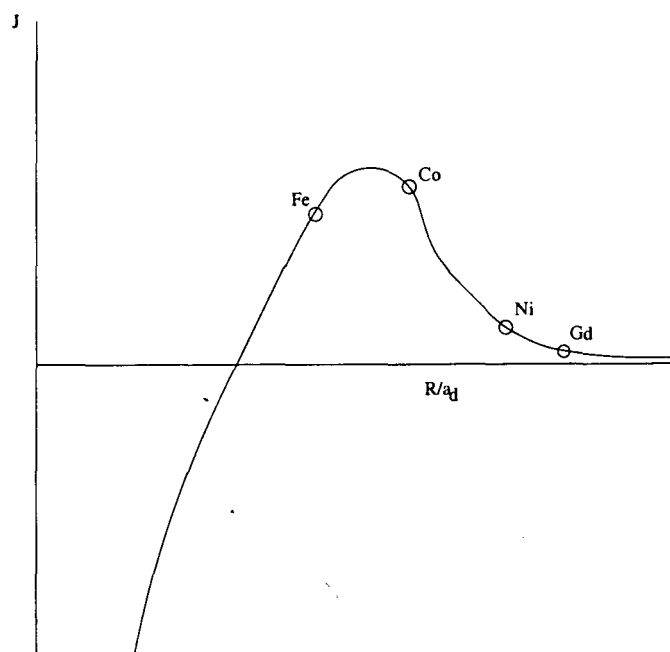


Figure 5.2: The interaction energy  $J$  as a function of  $r$ .  $r$  is the ratio of the interatomic distance to the diameter of the unfilled  $d$  shell

## 5.4 Pressure dependence of the Curie temperature in $Fe_{73.5}Cu_1Nb_3B_9Si_{12}$ and $Co_{65}Fe_5Mo_2B_{12}Si_{16}$

### 5.4.1 Experimental

The Curie temperature of  $Fe_{73.5}Cu_1Nb_3B_9Si_{12}$  and  $Co_{65}Fe_5Mo_2B_{12}Si_{16}$  was determined as a function of temperature at different pressures using the technique of ac calorimetry described in chapter 3. The sample was enclosed in Talc and placed in a Pyrophyllite cell. Talc was chosen as the pressure transmitting medium as its thermal conductivity ( 0.733 W/m/K ) is less than that of Pyrophyllite (6.8 W/m/K) . This minimizes the heat lost to the surroundings. The details about the cell assembly are given in chapter 2.

However the condition  $\omega^2\tau^2 \gg 1$  is no longer valid for pressures beyond 2 kbars. Consequently we cannot use the simple Eq. 3.11, instead we have to deal with Eq. 3.7. Since we are interested in the temperature variation of the specific heat, we require information on the temperature variation of the thermal conductivity to use Equation 3.7. Unfortunately this information is not available in the literature. Hence the behaviour of  $AT_c$ , obtained at higher pressures may not be a true reflection of the specific heat variation . However at the present moment we were only interested

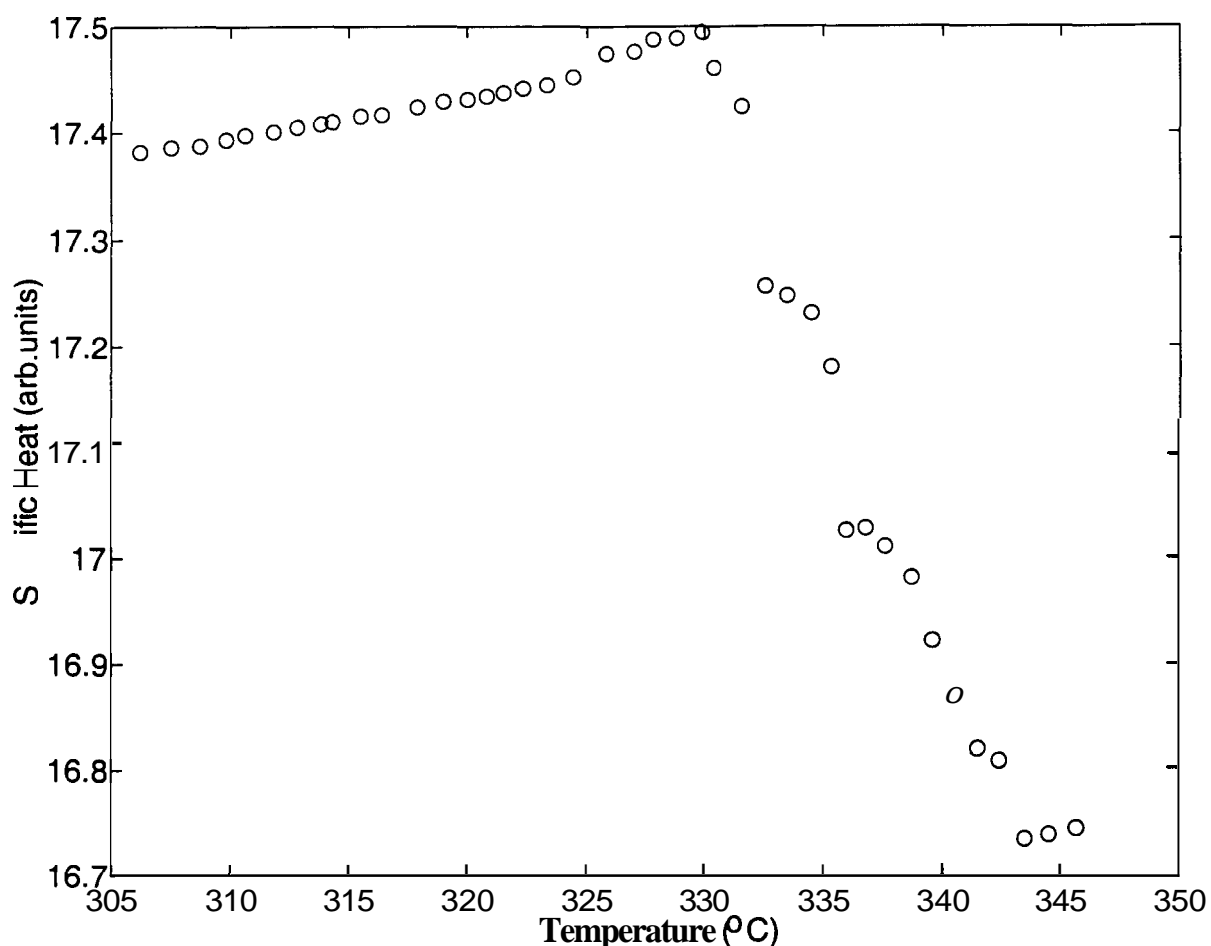


Figure 5.3: Specific Heat of  $Fe_{73.5}Cu_1Nb_3B_9Si_{12}$  at atmospheric pressure

in studying the Curie temperature as a function of pressure. We are still able to track the change in specific heat at the critical point up to a pressure of 20 kbar. Previous ac calorimetric techniques have not reached such pressures as they used a gas as the pressure transmitting medium [7]. Fig. 5.3 shows the specific heat of the metallic glass at atmospheric pressure. The change in the specific heat at the Curie temperature is clearly seen from this graph. We use this feature to track the Curie point transition, as the pressure is increased.

The high pressure specific heat measurements were done without a simultaneous measurement of the sample resistance. The simultaneous measurement of the sample resistance requires 6 leads to be taken out of the high pressure cell, whereas with the high pressure arrangement available to us we could only take out 4 leads through

the ceramic tube. The sample resistance was measured by a separate experiment using the ac resistivity technique [8]

The simultaneous measurement of the resistance is very important in the case of metallic glasses as the resistance of metallic glasses can be history dependent [9, 10]. However after one or two heating and cooling runs the resistance is fairly reversible. Hence in this case the simultaneous measurement of the resistance is not very important.

### 5.4.2 Discussion

The variation of the Curie temperature of  $Fe_{73.5}Cu_1Nb_3B_9Si_{12}$  is shown in Fig. 5.4. The Curie temperature of this metallic glass is around  $320^\circ C$  at atmospheric pressure. On application of pressure, the Curie temperature reduces from this value. Initially,  $dT_c/dP$  is quite small, but beyond 2 kbars it increases to about  $9^\circ C/kbar$ .

The experimental results seem to fit Eq. 5.21. This supports Wohlfarth's itinerant electron model.

$dT_c/dP$  for  $Fe_{73.5}Cu_1Nb_3B_9Si_{12}$  is found to be much greater than that for the other glass which was studied,  $Co_{65}Fe_5Mo_2B_{12}Si_{16}$ . In the case of the latter  $dT_c/dP$  is only of the order of  $2^\circ C/kbar$ . A high value of  $dT_c/dP$  is a characteristic of the Invar alloys. The 'Invar' behaviour has been observed in both crystalline and amorphous systems.

'Invar' is a short form for invariant. Alloys of Nickel and Iron which have a very low coefficient of thermal expansion come under this category. This kind of behaviour was first noticed in an alloy which had 65 % Iron and 35% Nickel. The first model which tried to explain the 'Invar' behaviour was the  $2\gamma$  model of Richard Weiss [11]. In this model it is assumed that Iron has two type of configurations, one in which the neighbouring spins are aligned parallel and one in which they are anti-parallel. It is conjectured that the parallel arrangement occupies a larger volume compared to the anti-parallel arrangement. This is due to the volume dependence of the magnetic interaction between the spins. The fact that the high density form of Iron is anti-ferromagnetic lends support to this theory.

As the temperature is increased the areas having anti-parallel spin arrangement grow at the expense of the parallel spin arrangement. The consequent decrease in volume makes up for the normal thermal expansion giving rise to a negligible net thermal expansion coefficient. Since the magnetic interactions are sensitive to volume changes, the Invar alloys also have a large pressure coefficient of the Curie

Chapter 4

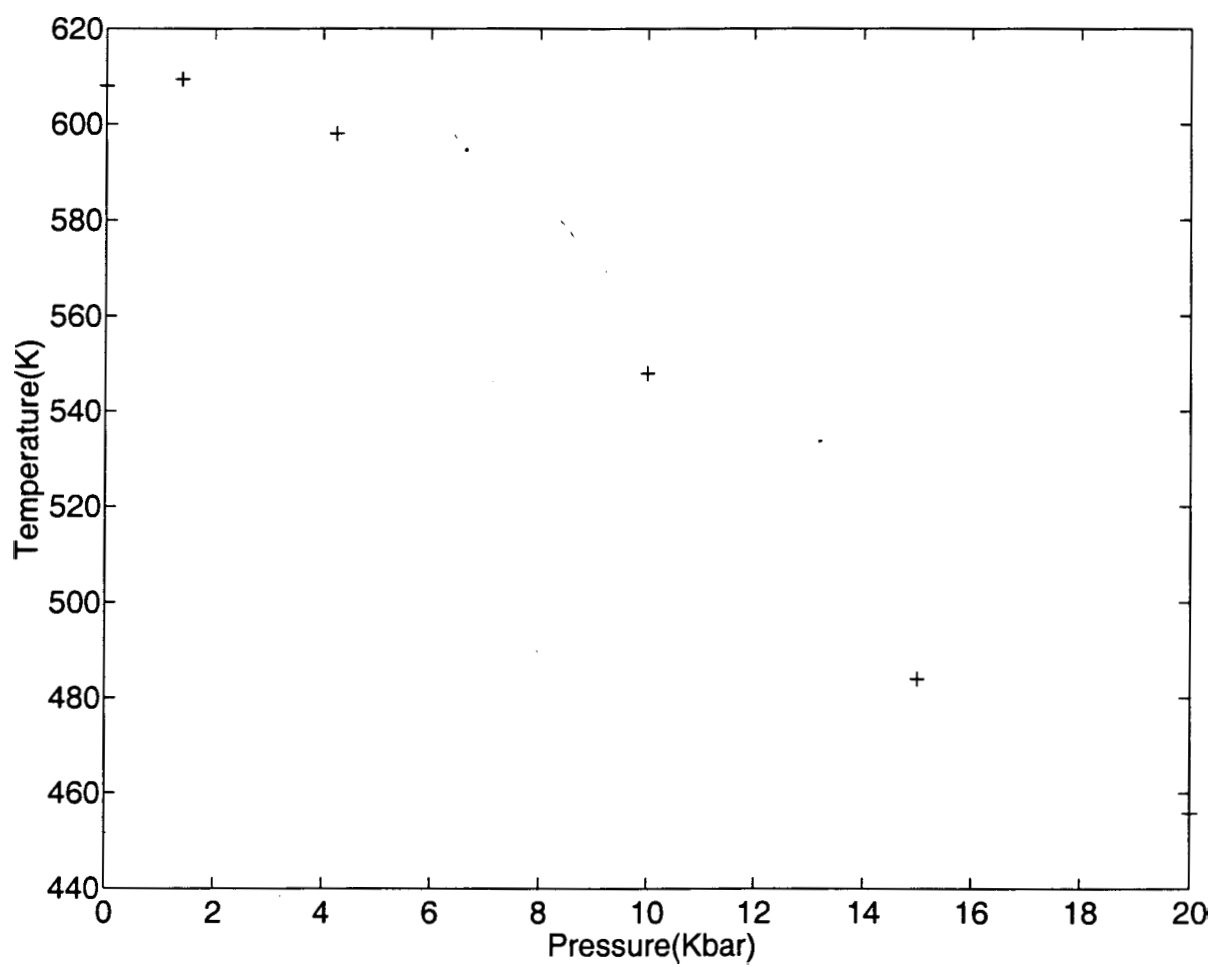


Figure 5.4: The Curie temperature of  $Fe_{73.5}Cu_1Nb_3B_9Si_{12}$  as a function of pressure

temperature.

Recently [12], the model of R. Weiss has been refined to include non-collinear spin arrangements, i.e, the spins are taken not just to be anti-parallel, but are likely to point to any direction. This model fits the experimental results more closely than the earlier model which assumes only anti-parallel spins.

It is interesting to compare the values of  $dT_c/dP$  for  $Fe_{73.5}Cu_1Nb_3B_9Si_{12}$  and  $Co_{65}Fe_5Mo_2B_{12}Si_{16}$  with values of  $dT_c/dP$  obtained for crystalline  $Fe$  and  $Co$ . In the case of  $Fe$  [13, 14] and  $Co$  [15],  $dT_c/dP$  is almost zero [16]. Addition of the metalloids seems to have made  $dT_c/dP$  negative and increased its magnitude. This effect is similar to the well-studied case of the crystalline Ni-Cu alloys [11], where  $dT_c/dP$  which is positive for Nickel decreases with addition of Copper and finally changes sign. This result is supportive of the minimum polarity model [17] rather than the rigid band model [18]. The rigid band model which assumes that the d-band fills up with the addition of Copper to Nickel, predicts an increase in  $dT_c/dP$ . Even though the rigid band model fails to predict the change in  $dT_c/dP$  with alloying, it seems to explain the transport properties quite well. In fact the rigid band model has been used to explain the transport properties (Chapter 4). This shows that no single model is able to explain all the available data in the itinerant magnetic systems.

We can also discuss the variation of  $T_c$  with pressure on the basis of the localized picture. For Iron and Cobalt, the value of 'J' corresponds to a point close to the peak in the J vs r curve (Fig. 5.2). Therefore  $dT_c/dP$  is almost close to zero as  $dJ/dr$  is almost close to zero. When Iron and Cobalt are alloyed with other elements to form the metallic glass, the diameter of the d-shell increases and hence 'r' shifts to a lower value. This leads to a reduction in 'J' (and hence  $T_c$ ) and also leads to a negative value for  $dT_c/dP$ . Since 'J' varies very sharply with 'r' for  $r < r_{peak}$ , the magnitude of  $dT_c/dP$  is quite high for Cobalt and Iron metallic glasses when compared to crystalline Nickel. However the localized model does not give a quantitative expression for  $dT_c/dP$  which can be tested against experiment.

### 5.4.3 Specific Heat studies on $Co_{65}Fe_5Mo_2B_{12}Si_{16}$

The specific heat curve for  $Co_{65}Fe_5Mo_2B_{12}Si_{16}$  at atmospheric pressure is shown in Fig. 5.5.

The parameters extracted out of fitting the specific heat data for  $Co_{65}Fe_5Mo_2B_{12}Si_{16}$  to Eq. 3.23 are:

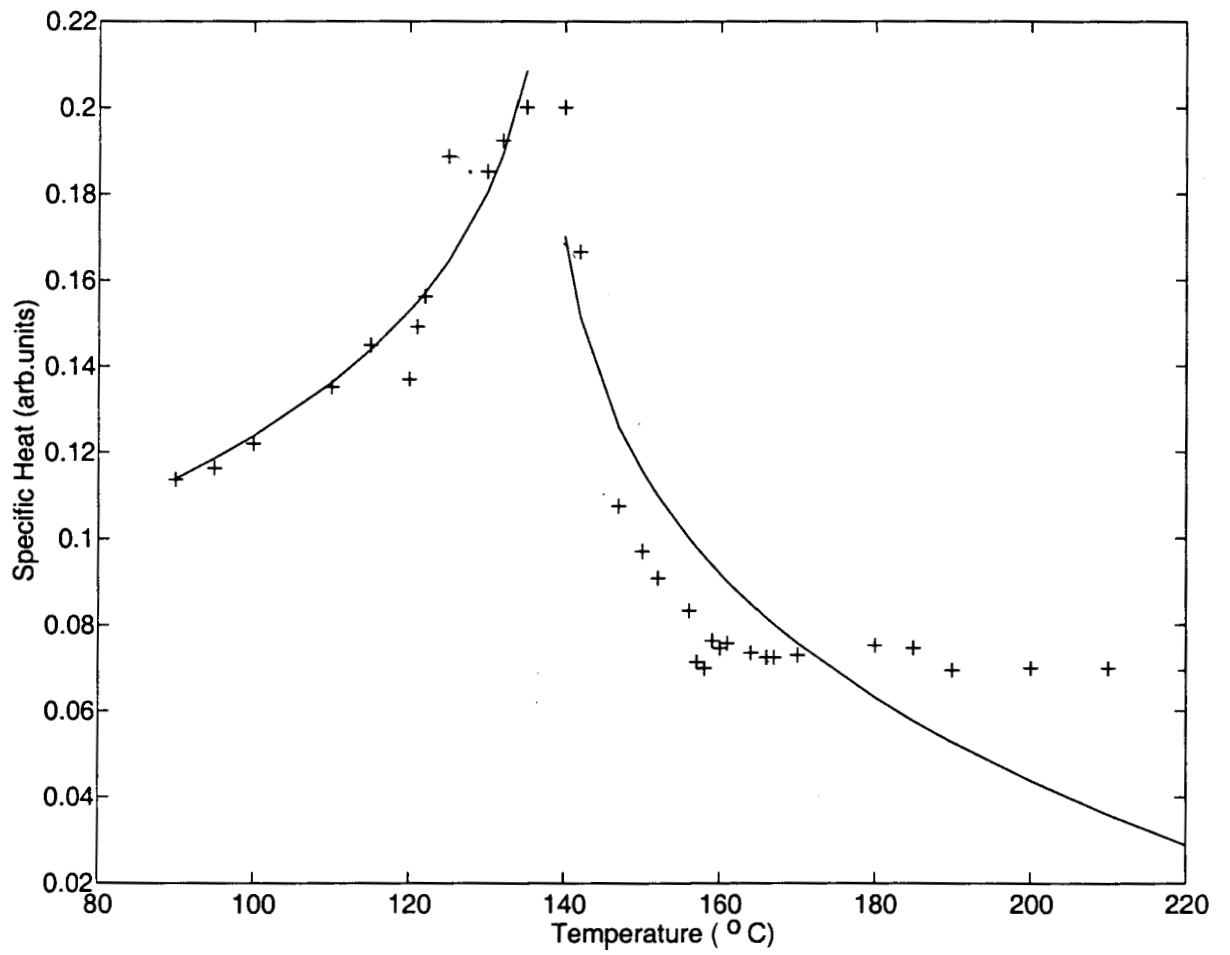


Figure 5.5: Specific heat of  $\text{Co}_{65}\text{Fe}_5\text{Mo}_2\text{B}_{12}\text{Si}_{16}$  at atmospheric pressure. '+' Experimental points, solid line is a fit to Eq. 3.23

$$T_c = 138.5 \pm 1$$

$$a = -0.2 \pm 0.05$$

$$A_+/A_- = 1.2$$

The value of the critical exponent which has been obtained, is slightly higher than the value  $-0.1$  which is expected for a Heisenberg system. Also the fit is not very good for  $T > T_c$ . Such deviations from the ideal critical exponent values have been reported in the past [19, 20]. However, when it is seen that the amplitude ratio exactly fits the Heisenberg model, it is not clear whether there are deviations from the ideal critical behaviour.

## 5.5 Conclusions

$dT_c/dP$  has been determined for the metallic glasses,  $Co_{65}Fe_5Mo_2B_{12}Si_{16}$  and  $Fe_{73.5}Cu_1Nb_3B_9Si_{12}$ .  $dT_c/dP$  is found to be around  $2^\circ C/kbar$  and  $9^\circ C/kbar$  respectively. The pressure dependence of the Curie temperature is consistent with the itinerant model. The Curie point transition could be traced up to a pressure of 20 kbars for the Fe-rich glass. The critical exponent for the specific heat of  $Co_{65}Fe_5Mo_2B_{12}Si_{16}$  was around  $-0.2$ , which is slightly higher than the value for the Heisenberg model. However the amplitude ratio was found follow the predictions of the Heisenberg model.

## References

- [1] Kanamori.J., Prog.theor.Phys. (Osaka) 30, 275(1963)
- [2] Hubbard J., Proc.phys.Soc., 84, 455(1964)
- [3] Heine, V., Phys.Rev., 153, 673(1967)
- [4] Chien,C.L. and Unruh,K.M., Phys.Rev., B24, 1556(1981)
- [5] E.P.Wohlfarth in Amorphous metallic *alloys*,p.283, Ed. by F.E.Luborsky, Butterworths, 1983
- [6] Moriya,T., J.Magn.Mag.Mat, 14, 1, 1979
- [7] Baloga and Garland,Rev.Sci.instrum, 48, 1977
- [8] V.Shubha and T.G.Ramesh, High temp.High Press., 18,311 (1986)
- [9] V.Shubha,T.G.Ramesh and A.K.Bhatnagar, 183,*Advances* in High pressure Science and technology, Ed. A.K. Singh, Tata McGraw-Hill, New Delhi 1995
- [10] K.V.Rao, page 401, Amorphous Metallic alloys, ed F.E.Luborsky, Butterworth and co ltd, 1983
- [11] R.Weiss, Proc.Roy.Soc. (London), 82, 281 (1963)
- [12] M. Van Schilfgarde, I.A.Abrikosov and B.Johansson, Nature, 100, 46 (1999)
- [13] Patrick, L., Phys.Rev. ,93, 384 (1954)
- [14] Leger, J.M., Susse, C. and Vodar, B., Sol.Stat.Comm., 4, 503 (1966)
- [15] Leger, J.M., Susse, C. and Vodar, B., Sol.Stat.Comm., 5, 755 (1967)
- [16] D.Bloch and A.S.Pavlovic, Advances in High Pressure Research Vol 3, Ed.R.S. Bradley, Academic Press, 1969

[17] J.H. Van Vleck, *Rev.Mod.Phys.*, 25, 220 (1953)

[18] N.F.Mott, *Proc.Phys.Soc (London)*, 47, 571 (1935)

[19] S.N. Kaul, *Phys.Rev.B*, 22, 278 (1980)

[20] Susumu Ikeda and Yoshikawa *J.Phy.Soc.Japan*, 49, 950 (1980)